A simple and precise way to determine electrical resistivity of isotropic conductors: Simplifying the four-probe method

Cite as: AIP Advances 13, 035134 (2023); doi: 10.1063/5.0139613
Submitted: 21 December 2022 • Accepted: 7 March 2023 •
Published Online: 28 March 2023

L. M. S. Alves,[1,2] F. S. Oliveira,[3] E. C. Romão,[1] M. S. da Luz,[4] and C. A. M. dos Santos[1,a)]

AFFILIATIONS

[1] Escola de Engenharia de Lorena, Universidade de São Paulo, Lorena-SP 12602-810, Brazil
[2] Instituto Federal de Educação, Ciência e Tecnologia Catarinense, Araquari-SC 89245-000, Brazil
[3] Instituto de Física "Gleb Wataghin," Universidade Estadual de Campinas, Campinas-SP 13083-970, Brazil
[4] Instituto de Ciências Tecnológicas e Exatas, Universidade Federal do Triângulo Mineiro, Uberaba-MG 38025-180, Brazil

[a)] **Author to whom correspondence should be addressed:** cams-eel@usp.br

ABSTRACT

Numerical simulations via COMSOL Multiphysics software are used to describe the behavior of electrical resistivity of several samples with rectangular shape typically used in the Montgomery method. The simulation data obtained using four isotropic conductors allowed us to understand in detail the behavior of the electric potential and electric field of the samples. The results provide an analytical method, which can substitute the four-probe method with much more simplicity and precision.

I. INTRODUCTION

The electrical resistivity (ρ) of a given material is one of the most important physical properties, and its correct determination has been the object of intense study during the last century.[1–5] This property has been used to classify materials into metals, semiconductors, insulators, and superconductors, which are the basis for electronic devices, such as resistors, capacitors, diodes, transistors, and many others.[6,7]

Several methods have been described for measuring electrical resistivity.[8–19] One of them was first described in 1915 by Wenner,[8] who tried measuring the electrical resistivity of the Earth with a method based on in-line four probes. The voltage drop V is measured between the two internal contacts, while an electrical current I is injected through the two external terminals. Later, this method was used to measure the electrical resistivity of a semiconductor wafer, being established as a reference procedure of the American Society for Testing and Materials Standards.[20] Nowadays, this method has been widely used to measure the electrical resistivity of conducting materials and it is well known as the conventional four-probe method (4P method).[1]

The 4P method is based on Ohm's law.[1] The four electrodes are usually arranged along one of the faces of a rectangular sample, as shown in Fig. 1, which must strictly respect some geometrical aspects.

Applying an electric field (E) to a conductor, an electric current (I) immediately appears and the electrical resistivity can be calculated from the ratio of the electric field and the current density ($J \equiv I/A$).[21] ρ is not directly determined in the experiments, but calculated after measuring the electrical resistance (R), which is obtained from the ratio of the measured voltage drop and the applied current.

The electrical resistivity is calculated by

$$\rho = R\frac{A}{l}, \tag{1}$$

where $A = wd$ is the cross section area of the specimen and l is the distance between the two points where the voltage drop is measured.

In order to have the precise determination of the electrical resistivity, the geometry of the sample and the electrical contacts must be well established. To measure the voltage drop, the electric field

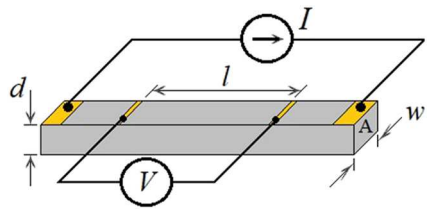

FIG. 1. Schematic view of the electrical contacts in the 4P method for a sample with rectangular shape, in which (i) the sample geometry must respect $\sqrt{A} \ll l$; (ii) the voltage contacts should be aligned perpendicular to the distance l; and (iii) the electrical current terminals must be large enough to have small contact resistances to avoid Joule self-heating.

must be approximately constant, which is obtained by cutting the sample with an aspect ratio that respects $\sqrt{A} \ll l$. The voltage contacts should be point or line-like (see Fig. 1), which must be perpendicular to the electrical field lines. Furthermore, both voltage and electrical current terminals must have very small contact resistance to avoid thermopower and Joule self-heating effects.

Although widely used, the 4P method has some limitations due to these experimental requirements. Samples of interest to be measured are usually in the millimeter size range and many times are not bars. In addition, electrical contacts cannot be prepared as pointed out earlier. These typical limitations always provide electrical resistivity measurements, which have errors as large as 10%–50%.[12,13]

In this work, the problem of measuring the electrical resistivity of isotropic samples of finite dimensions using the four-probe techniques has been revisited. Our previous experience measuring transport properties of isotropic and anisotropic samples leads us to modify the Montgomery and the van der Pauw methods.[17,18] Those works allowed us to find ways to calculate the electrical resistivity of both isotropic and anisotropic samples analytically. However, in order to understand these methods deeper, we intend to apply them to several sample geometries of different conducting materials. This is not a simple experimental task. We have noticed that this could be done by using numerical simulations. This work reports our first simulation results obtained from COMSOL Multiphysics software for rectangular thin samples using the Montgomery method. The simulations connected with our previous experimental experience in using the Montgomery and van der Pauw methods for measuring the electrical resistivity of both isotropic and anisotropic conductors (see Refs. 17 and 18) provide a method, which is simpler and more precise than the 4P method.

II. METHODOLOGY

COMSOL Multiphysics software was used to carry out all the simulations shown in this work.[22] This commercial software is much used for numerical projects in several knowledge areas, such as electric field, heat and mass flow, fatigue, and environmental studies.[23–28]

We have solved the problem of two-dimensional (2D) stationary electrical currents in conductive media, considering the equation of continuity in a stationary coordinate system, based on Ohm's law, which states that

$$J = \sigma E + J_e, \tag{2}$$

where σ is the electrical conductivity (in S/m), E is the electric field (in V/m), and J_e is an externally generated current density (in A/m^2), which is taken zero in the simulations. In such a case, the static form of the equation of continuity is given by

$$\nabla \cdot J = -\nabla \cdot (\sigma \nabla V) = 0. \tag{3}$$

The boundary conditions adopted a thin rectangular domain with dimensions $-L_1/2 \le x \le L_1/2$, $0 \le y \le L_2$, and thickness $L_3 = 1$ m, which respects $L_3 < \sqrt{L_1 L_2}$. Thus, the boundary conditions were determined in the following way:

$$V_A = V(-L_1/2, L_2) = -100 \text{ V}, \tag{4a}$$

$$V_B = V(L_1/2, L_2) = 100 \text{ V}, \tag{4b}$$

and for any other point in the boundary, the simulations took

$$n \cdot J = 0, \tag{4c}$$

where n is the normal vector at the surface boundary.

In the COMSOL software, the distributions of electric field lines as well as equipotential lines were easily simulated and the values of the V, E, I, and J as a function of the positions were recorded. Some schematic 2D views of the equipotential and electric field lines were also obtained. For example, Fig. 2(a) displays these lines for a typical isotropic conductor with rectangular thin geometry.

To verify the distribution of the equipotential and electric field lines across the samples, the electric potentials of −100 and +100 V [Eqs. (4a) and (4b)] were used in the A and B poles, as shown in Fig. 2. They simulated the application of the electrical current in both poles as done in the Montgomery experiments [see Fig. 2(b)], whose value is adjusted by the applied voltage ($V = V_B - V_A = 200$ V) and the electrical resistance of the samples,

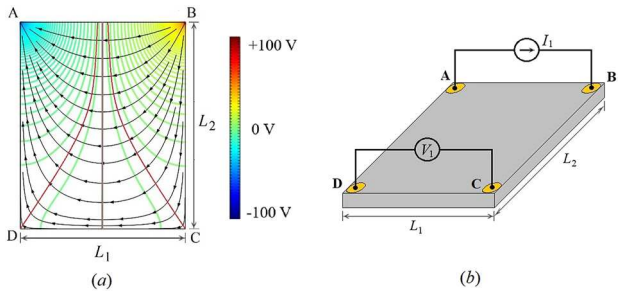

FIG. 2. (a) Typical schematic 2D view of the equipotential and electric field lines for a rectangular isotropic thin sample of dimensions L_1 and L_2 obtained using COMSOL Multiphysics software. The input electric potentials are applied at the A and B poles, and the output voltage is measured at C and D corners. The scale with color represents the voltage change over the entire simulated area. The highlighted vertical gray line represents the zero equipotential line (at $x = 0$), which divides the rectangular sample into two symmetric parts. The other two red lines touching the points C = $(L_1/2, 0)$ and D = $(-L_1/2, 0)$ are equipotential lines, which provide $V_1 = V_C - V_D$, which is crucial for the Montgomery method. (b) The typical sample geometry used in the Montgomery method.

which depends on the electrical resistivity of the conducting material and the geometrical parameters L_1, L_2, and L_3.

III. RESULTS AND DISCUSSION

Figure 3 displays the electric potential (V) and electric field (E) for four rectangular thin samples with different aspect ratios L_1 and L_2. The values of the potential and electric field were collected by performing a sweep around the A–D–C–B path shown in Fig. 2(a).

Near the negative and positive poles (A and B corners) the values of electric fields and potentials vary strongly as a function of the position. On the other hand, on the opposite side of the samples (D–C path), both V and E are orders of magnitude smaller. Furthermore, it is observed that the shape of the curve for the different sizes is very similar and can be easily collapsed (not shown).

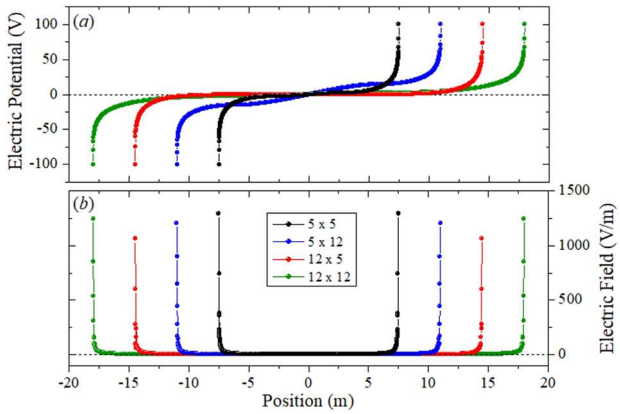

FIG. 3. Electric potential (V) (a) and electric field (E) (b) as a function of position along the A–D–C–B path for four rectangular thin samples with different aspect ratios L_1 and L_2. The origin was defined at the midpoint of the D–C line. The values of the potential and electric field were collected by performing a sweep around the A–D–C–B path shown in Fig. 2(a).

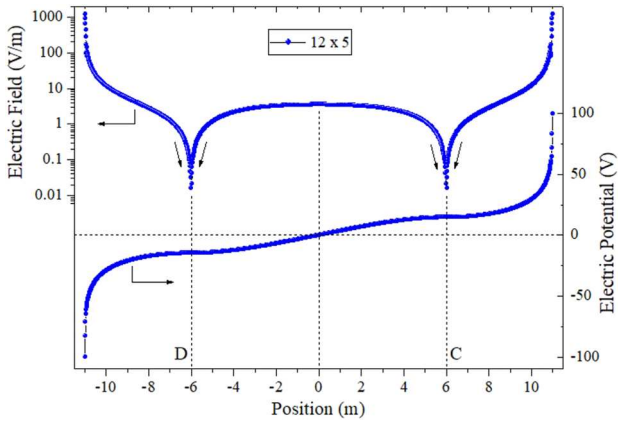

FIG. 4. Electric field (upper curve) and electric potential (lower curve) along the A–D–C–B path for the sample with L_1 = 12 m and L_2 = 5 m.

Figure 4 shows the electric field and electric potential in logarithm scales for the A–D–C–B path of the sample with L_1 = 12 m and L_2 = 5 m.

The electric field (upper curve) is related to electric potential (lower curve) by $\vec{E} = -\nabla V$. It interesting to note that the electric potential has saddle points at corners C and D, where the electric field vanishes (see arrows). At the middle point of the D–C path (x = 0), the electric potential is maximum and the electrical potential is zero, as expected due to the symmetric arguments. The same general behavior has been observed for all the simulated samples.

To have a deep insight into the electric behavior in the D–C path, the electric potential for the four samples is plotted in Fig. 5.

Considering the zero electric potential at $x = 0$ and the two saddle points at $x = \pm L_1/2$, the behavior of the $V(x)$ must be described by a third-order polynomial, whose boundary conditions impose that

$$V(x) = \frac{V_1}{2}\left(3\frac{x}{L_1} - 4\frac{x^3}{L_1^3}\right). \quad (5)$$

Figure 5 also displays the fits based on Eq. (5) (red solid lines). The agreement is excellent and allows one to determine the

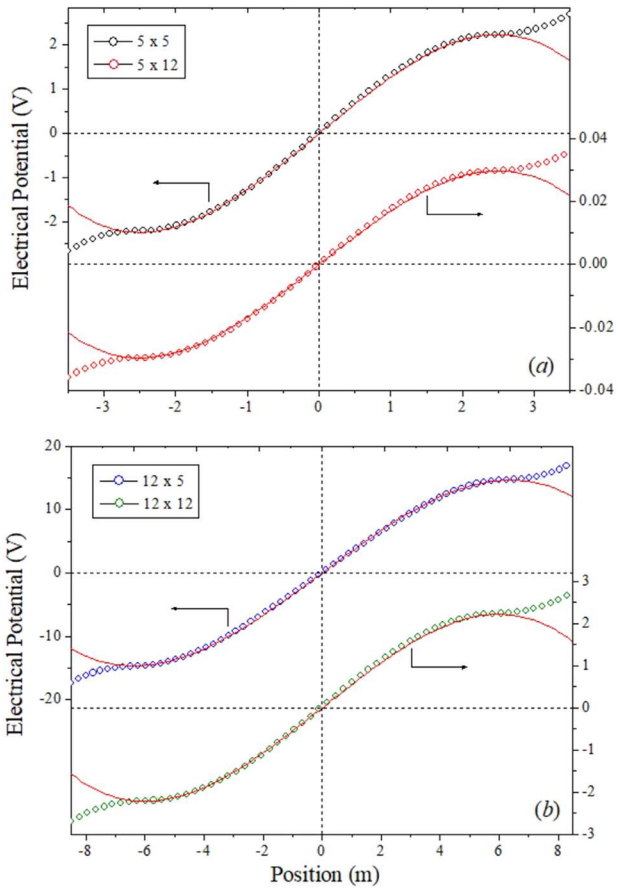

FIG. 5. Electric potential along the D–C path for the samples with (a) $L_1 \times L_2$ = 5 × 5 and 5 × 12, and (b) $L_1 \times L_2$ = 12 × 5 and 12 × 12. Red solid lines are fits based on Eq. (5).

$V_1 = V_C - V_D$ value for each sample with high precision either by using the polynomial fit or from the saddle points.

In Fig. 6 is shown a set of electric potential curves as a function of the position for samples with a fixed D–C distance (L_1 = 5 m) and different L_2.

It is easy to notice that the saddle points are in the same position for all the samples as indicated by the small black solid circles at $x = \pm 2.5$ m. Similar behaviors have been observed for samples with different L_1 values, which demonstrate that this is a general behavior of the rectangular samples in the Montgomery method.[14] As previously mentioned, this would be difficult to be performed experimentally. Thanks to COMSOL Multiphysics software, which allowed us to do this type of simulation for many samples very fast.

As reported in a previous paper,[14,17] there is a simple relationship between the thin rectangular sample and its electrical resistance. This is given in the modified Montgomery method [see Eq. (10) of Ref. 17] by

$$\rho = (\pi/8) L_3 R_1 \sinh(\pi L_2/L_1), \tag{6}$$

where $R_1 = V_1/I_1$ is the sample resistance in the Montgomery method and L_3 is the samples thickness. Interesting is the behavior expected for a square sample ($L_1 = L_2$), in which the sheet resistance is given by

$$\rho/L_3 = 4.535\, R_1. \tag{7}$$

In order to check the validity of the simulation data obtained in this work with regard to Eq. (6), in Fig. 7(a) are plotted the V_1 values obtained as described in Fig. 5 as a function of the $1/\sinh(\pi L_2/L_1)$ in the limit $L_2/L_1 \geq 0.5$ for four different metallic materials (Cu, Al, Pt, and Hg). For this particular case, a constant electrical current of 1 A was used in the simulations of the thin samples (L_3 = 1 m).

The linear behavior observed in both log–log (main panel) and linear (inset) scales in Fig. 7(a) for all the metals unambiguously demonstrates that Eq. (6) describes the simulated data pretty well. Furthermore, plotting the electrical resistivity as a function of the slope obtained from the inset of Fig. 7(a), as displayed in Fig. 7(b), shows an excellent agreement with pre-factor $(\pi/8)$ predicted in Eq. (6).

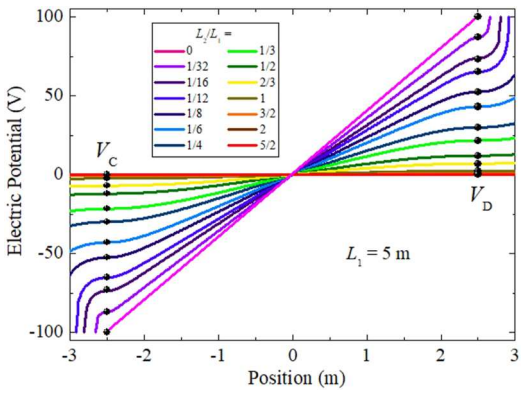

FIG. 6. Electric potential curves as a function of the position for samples with a fixed *D–C* distance (L_1 = 5 m) and different L_2.

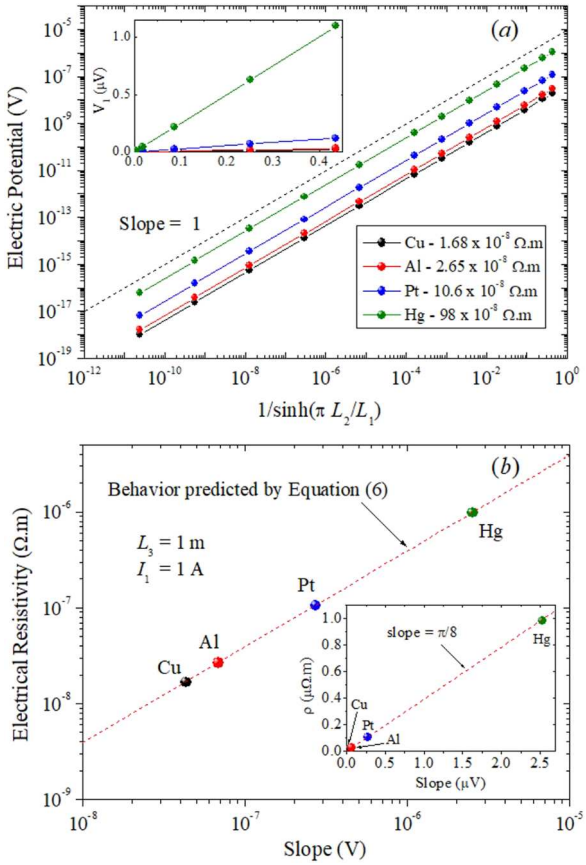

FIG. 7. (a) V_1 (electric potential) as a function of the $1/\sinh(\pi L_2/L_1)$: The values were obtained as described in Fig. 5 for the limit $L_2/L_1 \geq 0.5$,using simulations with a constant electrical current of 1 A. The inset shows the same curve in linear scale. (b) Electrical resistivity of four metals as a function of the slope obtained from the inset of (a). The inset displays the same curve in linear scale, where the slope is equal to $\pi/8$. The red dotted lines represent the behavior predicted by Eq. (6).

Finally, we have noticed that the results shown in this work allow us to suggest a simple and precise method for determining the electrical resistivity of isotropic conductors, especially when the sample is like a thin rectangular block (L_1 is comparable to L_2 and $L_3 \ll \sqrt{L_1 L_2}$). In such a case, the following advantages have been observed with regard to the conventional 4P method: (*i*) contacts can be placed at the corners of the samples becoming easier to handle and avoiding short circuits; and (*ii*) precision to determine electrical resistivity can be improved since the samples can be bigger and contact smaller than in the 4P method, as well as avoids misorientation in the contacts. One additional important measurement aspect has to do with the square sample ($L_1 = L_2$). Preparing the sample directly in a square shape or cutting it in such a shape provides the easiest way to determine the electrical resistivity, which is directly calculated by Eq. (7) and square size independent.

To check the method proposed here, the experimental data reported previously for copper plates and aluminum foils (see Ref. 17) were compared with the sheet resistance (ρ/L_3) predicted by

Eq. (6). The agreement is excellent, demonstrating that it is easy to use Eq. (6) or (7) for determining the electrical resistivity of isotropic samples.

IV. CONCLUSIONS

This work provides a simple method for measuring the electrical resistivity of rectangular isotropic samples. The simulation using COMSOL Multiphysics software allowed us to study the Montgomery method in much more detail never reported before. The simulations proved that the analytical method previously reported can be used in many practical situations. The results show that the method reported here can be easily used in substitution to the conventional four-probe method.

ACKNOWLEDGMENTS

L. M. S. Alves is a post-doc at EEL-USP (Proc. 21.1.419.88.8). F. S. Oliveira is a post-doc at UNICAMP (FAPESP Grant No. 2021/03298-7). M. S. da Luz is a CNPq fellow (Proc. 311394/2021-3). This material is based upon support by CAPES (Proc. 23038.000263/2022-19).

AUTHOR DECLARATIONS

Conflict of Interest

The authors have no conflicts to disclose.

Author Contributions

L. M. S. Alves: Investigation (equal); Methodology (equal); Writing – review & editing (equal). **F. S. Oliveira**: Conceptualization (equal); Formal analysis (equal); Methodology (equal); Software (equal); Writing – original draft (equal); Writing – review & editing (equal). **E. C. Romão**: Conceptualization (equal); Formal analysis (equal); Methodology (equal); Software (equal); Writing – original draft (equal); Writing – review & editing (equal). **M. S. da Luz**: Conceptualization (equal); Formal analysis (equal); Methodology (equal); Writing – original draft (equal); Writing – review & editing (equal). **C. A. M. dos Santos**: Conceptualization (equal); Methodology (equal); Writing – original draft (equal); Writing – review & editing (equal).

DATA AVAILABILITY

The data that support the findings of this study are available from the corresponding author upon reasonable request.

REFERENCES

[1] I. Miccoli, F. Edler, H. Pfnür, and C. Tegenkamp, "The 100th anniversary of the four-point probe technique: The role of probe geometries in isotropic and anisotropic systems," J. Phys.: Condens. Matter **27**, 223201 (2015).
[2] Y. J. Yun, H. Y. Yu, and D. Han Ha, "Measurement of electrical transport along stretched λ-DNA molecules using the four-probe method," Curr. Appl. Phys. **11**, 1197 (2011).
[3] S. Matsuo and N. R. Sottos, "Single carbon fiber transverse electrical resistivity measurement via the van der Pauw method," J. Appl. Phys. **130**, 115105 (2021).
[4] F. Keywell and G. Dorosheski, "Measurement of the sheet resistivity of a square wafer with a square four-point probe," Rev. Sci. Instrum. **31**, 833 (1960).
[5] M. G. Buehler and W. R. Thurber, "Measurement of the resistivity of a thin square sample with a square four-probe array," Solid-Stale Electron. **20**, 403 (1977).
[6] B. L. Theraja and R. S. Sedha, *Principles of Electronic Devices and Circuits* (S. Chand Publishing, 2007).
[7] S. M. Sze and K. K. Ng, *Physics of Semiconductor Devices* (Wiley, Hoboken, NJ, 2007).
[8] F. Wenner, "A method of measuring Earth resistivity," Bull. Bur. Stand. **12**, 469 (1915).
[9] L. B. Lugansky and V. I. Tsebro, "Four-probe methods for measuring the resistivity of samples in the form of rectangular parallelepipeds," Instrum. Exp. Tech. **58**, 118 (2015).
[10] I. Kazani, G. De Mey, C. Hertleer, J. Banaszczyk, A. Schwarz, G. Guxho, and L. Van Langenhove, "Van Der Pauw method for measuring resistivities of anisotropic layers printed on textile substrates," Text. Res. J. **81**(20), 2117 (2011).
[11] W. Versnel, "Electrical characteristics of an anisotropic semiconductor sample of circular shape with finite contacts," J. Appl. Phys. **54**, 916 (1983).
[12] L. J. van der Pauw, Philips Res. Rep. **13**, 1 (1958).
[13] L. J. van der Pauw, Philips Tech. Rev. **20**, 220 (1958).
[14] H. C. Montgomery, "Method for measuring electrical resistivity of anisotropic materials," J. Appl. Phys. **42**, 2971 (1971).
[15] B. F. Logan, S. O. Rice, and R. F. Wick, "Series for computing current flow in a rectangular block," J. Appl. Phys. **42**, 2975 (1971).
[16] J. D. Wasscher, "Note on four-point resistivity measurements on anisotropic conductors," Philips Res. Rep. **16**, 301 (1961).
[17] C. A. M. dos Santos, A. de Campos, M. S. da Luz, B. D. White, J. J. Neumeier, B. S. de Lima, and C. Y. Shigue, "Procedure for measuring electrical resistivity of anisotropic materials: A revision of the Montgomery method," J. Appl. Phys. **110**, 083703 (2011).
[18] F. S. Oliveira, R. B. Cipriano, F. T. da Silva, E. C. Romão, and C. A. M. dos Santos, "Simple analytical method for determining electrical resistivity and sheet resistance using the van der Pauw procedure," Sci. Rep. **10**, 16379 (2020).
[19] S. H. N. Lim, D. R. McKenzie, and M. M. M. Van der Bilek, "van der Pauw method for measuring resistivity of a plane sample with distant boundaries," Rev. Sci. Instrum. **80**, 075109 (2009).
[20] ASTM 1975 Annual Book of ASTM Standards part 43, F84.
[21] R. A. Serway, *Principles of Physics* (Saunders College Publishing, London, 1998).
[22] COMSOL™ 5.1 Multiphysics, Reference Manual, 2015.
[23] J. Lin, P. Y. Wong, P. Yang, Y. Y. Lau, W. Tang, and P. Zhang, "Electric field distribution and current emission in a miniaturized geometrical diode," J. Appl. Phys. **121**, 244301 (2017).
[24] A. I. Sharshir, S. A. Fayek, Amal. F. Abd El-Gawad, M. A. Farahat, M. I. Ismail, and Mohamed Mohamady Ghobashy, "Experimental investigation of E-beam effect on the electric field distribution in cross-linked polyethylene/ZnO nanocomposites for medium-voltage cables simulated by COMSOL Multiphysics," J. Anal. Sci. Technol. **13**, 16 (2022).
[25] P. Song, Q. Song, Z. Yang, G. Zeng, H. Xu, X. Li, and W. Xiong, "Numerical simulation and exploration of electrocoagulation process for arsenic and antimony removal: Electric field, flow field, and mass transfer studies," J. Environ. Manage. **228**, 336 (2018).
[26] J. Furlan, J. A. Martins, and E. C. Romão, "Dispersion of toxic gases (CO and CO_2) by 2D numerical simulation," Ain Shams Eng. J. **10**, 151 (2019).
[27] C. A. Perussello, C. Kumar, F. de Castilhos, and M. A. Karim, "Heat and mass transfer modeling of the osmo-convective drying of yacon roots (*Smallanthus sonchifolius*)," Appl. Therm. Eng. **63**, 23 (2014).
[28] M. Daş, E. Alıç, and E. K. Akpinar, "Numerical and experimental analysis of heat and mass transfer in the drying process of the solar drying system," Eng. Sci. Technol., Int. J. **24**, 236 (2021).